Evolution of particle size distributions in crushable granular materials

Duc-Hanh Nguyen, Philippe Sornay, Emilien Azéma, Farhang Radjai

Evolution of particle size distributions in crushable granular materials

Duc-Hanh Nguyen, Philippe Sornay
CEA, DEN, DEC, SPUA, LCU
F-13108 Saint Paul lez Durance, France.

Emilien Azéma, Farhang Radjai
University Montpellier 2, CNRS
LMGC, Place Eugène Bataillon, 34095 Montpellier Cedex 05, France.

ABSTRACT: By means of the contact dynamics method together with a particle fracture model, in which the particles are cohesive aggregates of irreducible polygonal fragments, we investigate the evolution of particle size distribution in the process of uniaxial compaction of granular materials. The case of single particle breakup under compressive stress is used to test the method and the influence of discretization (number of irreducible fragments). We show that the breaking threshold of the granular assembly scales with the internal cohesion of the particles but it depends also on the initial size distribution and irregularity of polygonal particle shapes. The evolution of size distribution proceeds by consecutive periods of intense particle crushing, characterized by local shattering instability, and periods of little breaking activity. Starting with either monodisperse or power-law distribution of particle sizes, the latter evolves towards a broad distribution of the fragmented particles with a nearly power-law distribution in the range of intermediate particle sizes. Interestingly, a finite number of large particles survive despite ongoing crushing process due to the more homogeneous distribution of forces in the presence of small fragmented particles filling the pores between larger particles.

1 INTRODUCTION

Particle breakage occurs very commonly in natural granular flows and in industrial processes involving the transport, handling and compaction of granular materials. The particle size reduction is often undesired or uncontrolled, and it is referred to as attrition process. In contrast, the fragmentation of particles under controlled conditions is used in comminution processes such as the milling of vegetal products or grinding of mineral materials. The evolution of particle size distribution and energy dissipation in such processes depend on many factors such as particle properties (shape, crushability), initial size distribution, loading history and mobility of the grains during the crushing process (Thornton, Yin, & Adams 1996, Fuerstenau, Gutsche, & Kapur 1996, Couroyer, Ning, & Ghadiri 2000, Potapov & Campbell 2001, Nakata, Hyodo, Hyde, Kato, & Murata 2001, Cleary 2001, Bolton, 2, & Cheng 2008, Hosten & Cimilli 2009, Liu, Kafui, & Thornton 2010).

The manufacture of compact shapes by molding powdered materials is the archetypal example of a process in which the bulk crushing of particles plays as much a role as particle rearrangements (Fuerstenau, Gutsche, & Kapur 1996, Hosten & Cimilli 2009, Das, Nguyen, & Einav 2011, Ben-Nun, Einav, & Tordesillas 2010, Esnault & Roux 2013). However, despite its industrial importance, the compaction process and its underlying microscopic mechanisms are still poorly understood partially due to short length and time scales governing particle breakup. The bulk comminution process and redistribution of the fragments during compaction are controlled by the structural disorder of granular media and highly inhomogeneous distribution of contact forces (Tsoungui, Vallet, Charmet, & Roux 1997, Radjaï 1998, Thornton, Ciomocos, & Adams 2004, Agnolin & Roux 2007, Ben-Nun, Einav, & Tordesillas 2010). Moreover, the process is both nonlinear and nonlocal as cascading events follow a local particle breakup and seem to have strong impact on the resulting size distributions (Esnault & Roux 2013). Analytical models have also been proposed for the distribution of particle sizes (Wohletz, Sheridan, & Brown 1989, Redner 1990, Astrom & Herrmann 1998, Gorokhovski 2003, Elek & Jaramaz 2009, Bird, Watts, Tarquis, & Whitmore 2009). Most models are based on kinematic considerations and the cascading nature of the fragmentation process, leading thus to log-normal distributions

or power laws. However, the nonlinear effects and homogeneity of breakup events inside the material are essential for the size distributions (Redner 1990, Bird, Watts, Tarquis, & Whitmore 2009).

Numerical simulations by the molecular dynamics (MD) or discrete element method (DEM) have been increasingly employed in order to get a better understanding of the particle-scale mechanisms of the comminution process (Thornton, Yin, & Adams 1996, Moreno, Ghadiri, & Antony 2003, Liu, Kafui, & Thornton 2010). Such methods combine the general framework of the DEM, based on rigid-body dynamics and frictional contact interactions, with a particle fracture model. DEM numerical models have the advantage of providing detailed information about the local particle environments and force chains that control the local breakup events. The most straightforward approach consists in modeling the particles as agglomerates of irreducible spherical particles bonded together by cohesive forces. Such agglomerates may represent real agglomerates such as pellets and ceramic compacts . This model has, however, been more generally used to investigate the behavior of crushable soils, rocks, fault gouge and other materials (Cheng, Bolton, & Nakata 2004, Khanal, Schubert, & Tomas 2007, Bolton, 2, & Cheng 2008, Abe & Mair 2009, Wang & Yan 2012, Timár, Kun, Carmona, & Herrmann 2012, Metzger & Glasser 2012). An alternative method consists in replacing a circular or spherical particle at its fracture threshold by several smaller fragments of the same shape (Astrom & Herrmann 1998, Tsoungui, Vallet, & Charmet 1999, Ben-Nun, Einav, & Tordesillas 2010). A major drawback of both methods is that an aggregate of spherical particles includes voids, so that the breakup of the agglomerate leads to volume loss. To circumvent this pathology, some authors have applied the DEM to particles of arbitrary shape discretized into polygons interconnected by springs with a breaking threshold (D'Addetta, Kun, & Ramm 2002, Galindo-Torres, Pedroso, Williams, & Li 2012). This approach has been used to study the fragmentation process of a single particle.

In this paper, we introduce a novel approach based on the contact dynamics (CD) method (Moreau 1994, Radjaï& Richefeu 2009, Radjaï& Dubois 2011). The particles have polygonal shapes and modeled as cohesive aggregates of irreducible fragments of polygonal shape generated by Voronoi tessellation so that they fill the whole volume of the particle. A contact line between two irreducible fragments loses its cohesion and becomes frictional when a cohesion threshold is reached. Upon fragmentation, the total volume of the fragments is equal to the initial volume of the initial particle, so that, in contrast with an aggregate of circular particles, the volume is conserved. As we shall see below, our simulations reveal the highly nonlinear feature of the breaking process with periods of intense breakup events followed by periods of loading with little breaking activity. We also observe local shattering of the particles as well as a finite number of surviving particles. The size distributions are rather complex as they can not be fitted into a single function, but we find that the intermediate sizes are rather well represented by power-law distributions.

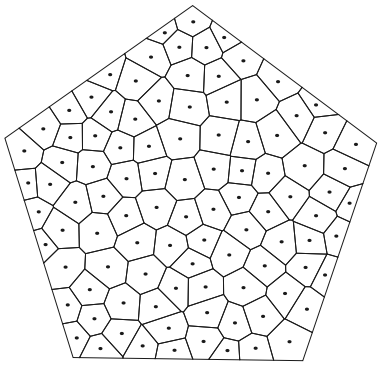

Figure 1: Discretization of a particle by Voronoi cells representing irreducible fragments interacting by cohesive forces.

In the following, we first describe the numerical procedures and our particle system. Then, we consider the case of single particle breakup in order to quantify the effect of discretization. Then, we present the evolution of size distributions for different system parameters as a function of the compressive stress. We conclude with a brief discussion of the most salient findings of this work.

2 NUMERICAL PROCEDURES

The simulations were carried out by means of the CD method, which is suitable for simulating large assemblies of undeformable particles (Moreau 1994, Radjaï& Richefeu 2009). In this method, the equations of motion are integrated by an implicit time-stepping scheme accounting for the kinematic constraints resulting from frictional contact interactions. The implicit integration scheme makes the method unconditionally stable. An iterative algorithm is used to determine the contact forces and particle velocities simultaneously for all particles in the system. The CD method has been extensively employed for the simulation of aspherical particles (Azéma, Radjaï, Peyroux, & Saussine 2007, Azéma, Radjaï, & Saussine 2009, Azéma & Radjaï 2010, Azéma & Radjaï 2012, Azéma, Radjaï, & Dubois 2013).

We divide each particle into irreducible fragments by Voronoi tessellation as shown in figure 1. These fragments represent primary rigid particles that interact by frictional cohesion along their sides characterized by a normal fracture threshold σ_c and a shear threshold $\mu_s\sigma_c$, where μ_s is the internal friction coefficient. All primary fragments interact by side/side contacts. The normal adhesion threshold f_c between two fragments linearly depends on the length L of the contact (representing the interface): $f_c = 0.5L\sigma_c$, where σ_c is the internal cohesion of the particle. The factor 0.5 accounts for the two contact points representing

geometrically a side/side contact. The fracture is assumed to be irreversible and a side/side contact transforming into a side/vertex contact loses its cohesion. Each contact point carries a normal force f_n and a tangential force f_t. The friction coefficient in the simulations reported below is set to $\mu_s = 0.3$.

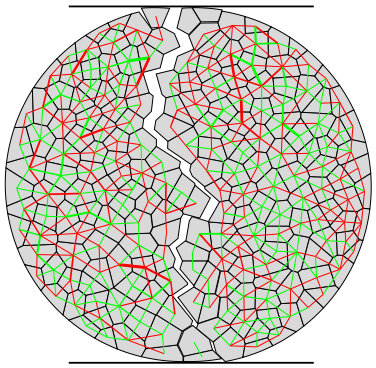

Figure 2: A single circular particle subjected to diametral compression. The red and green lines represent compressive and tensile contacts, respectively.

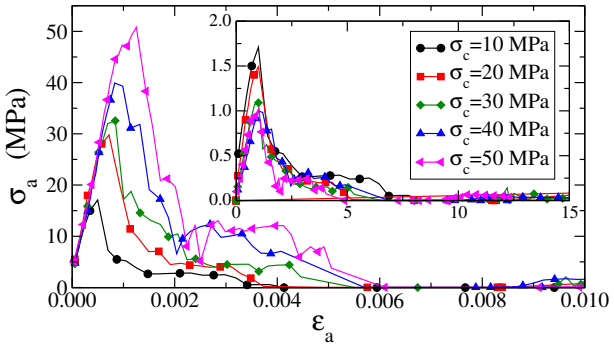

Figure 3: Axial stress versus axial strain for several values of the cohesive stress σ_c. The inset shows the axial stress normalized by σ_c.

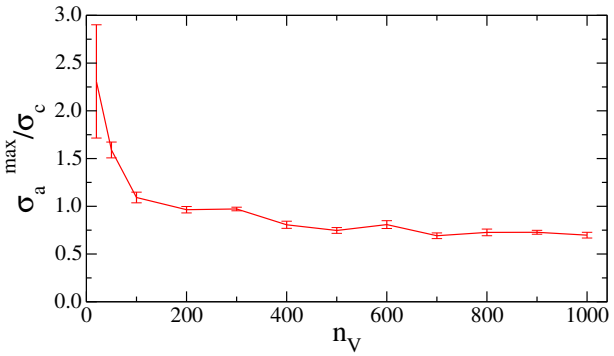

Figure 4: Tensile strength normalized by the internal cohesion as a function of the number n_V of Voronoi cells.

We used slow single-particle compression tests in order to evaluate the effect of numerical parameters on the breakup process. Fig. 2 displays the incipient fracture of a particle compressed between two planes together with compressive and tensile forces between irreducible fragments composing the particle. The crack is triggered at the top plane and propagates from top to bottom into the particle. This mode-I fracture is observed in experiments. The zigzag aspect of the main crack reflects the rather coarse discretization of the particle. We also observe secondary cracks, and small fragments in addition to the two main fragments produced.

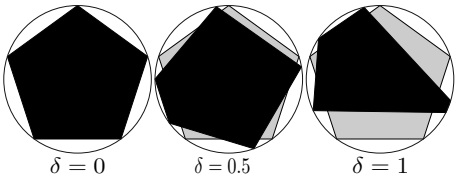

Figure 5: Example of a regular pentagon $\delta = 0$ transformed into irregular pentagons for two values of the parameter δ (see text).

Figure 3 shows the mean axial stress σ_a as a function of axial deformation ε_a for different values of the internal cohesion σ_c. The stress increases smoothly with strain and falls off abruptly when fracture is triggered. The stress peak is the fracture threshold of the particle. Except for the lowest cohesion, it scales with σ_c, as shown in the inset. The higher threshold of σ_a/σ_c in the low-cohesion limit may be attributed to the prevailing effect of interlocking and friction between fragments as compared to the cohesive interactions. This is consistent with the fact that the fracture threshold σ_a^{max} declines when the number n_V of meshing Voronoi cells increases, as shown in Fig. 4. For $n_V > 100$ the fracture threshold is nearly independent of n_V, indicating that for $n_V > 100$ the details of Voronoi tessellation do not affect the fracture behaviour of the particle. In the simulations reported below all particles, irrespective of their sizes, are meshed with irreducible fragments of the same size and the smallest particles have at least 50 fragments.

3 EVOLUTION OF SIZE DISTRIBUTIONS IN UNIAXIAL COMPRESSION

We consider the evolution of particle size distributions of an assembly of polygonal particles in oedometric geometry. We use pentagons as reference particle shape. An irregular pentagon can be obtained by changing the angular positions of the vertices. Let θ_0 be the position of the first vertex. The angular position of a vertex i is given by $\theta^i = \theta_0 + 2\pi i/5$. This regular pentagon can be transformed into an irregular pentagon by perturbing randomly the position of each vertex i within an angular limit $\pm\delta\pi/5$: $\theta^i = \theta_0 + \frac{2\pi}{5}i \pm \delta\frac{\pi}{5}$, where δ can be varied in the range $[0, 1]$. Its value quantifies the degree of shape irregularity. Fig. 5 shows two examples of irregular pentagons constructed from a regular one. The size of a pentagonal particle is defined by the diameter d of its circumscribed disk. It is varied in a range $[d_{min}, d_{max}]$ with a uniform distribution of particle volume fractions. Following (Voivret, Radjaï, Delenne, & Youssoufi 2007), we define the size span s of the distribution by $s = \frac{d_{max}-d_{min}}{d_{max}+d_{min}}$. The value $s = 0$ corresponds to

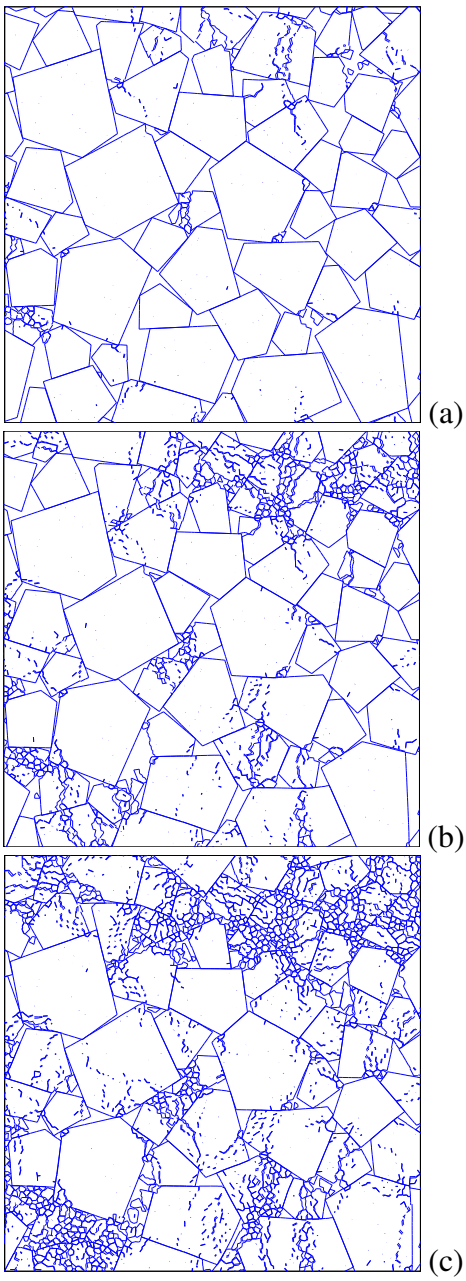

Figure 6: Three snapshots of a packing under uniaxial compaction for axial stresses $\sigma_a = \sigma_c$(a) $\sigma_a = 2\sigma_c$(b) and $\sigma_a = 10\sigma_c$(c).

a monodisperse packing whereas $s = 1$ corresponds to "infinite" polydispersity.

All packings are prepared according to the same protocol. For given values of s and δ, 200 particles are generated with ten size classes and a uniform particle volume distribution. The particles are initially placed on a square network in a rectangular box of dimensions $l_0 \times h_0$ and deposited under the action of the gravity g. Then, the gravity is set to 0 and the packings are subjected to vertical compression under an axial load σ_a applied on the upper wall and where the left, bottom and right walls are fixed. The friction coefficient between particles and with the walls is set to zero during the compression in order to obtain dense and nearly isotropic packings. The compression is stopped when the contact force network jams. The samples prepared by the above procedure are then subjected to to uniaxial compaction in the same box by incrementally increasing σ_a.

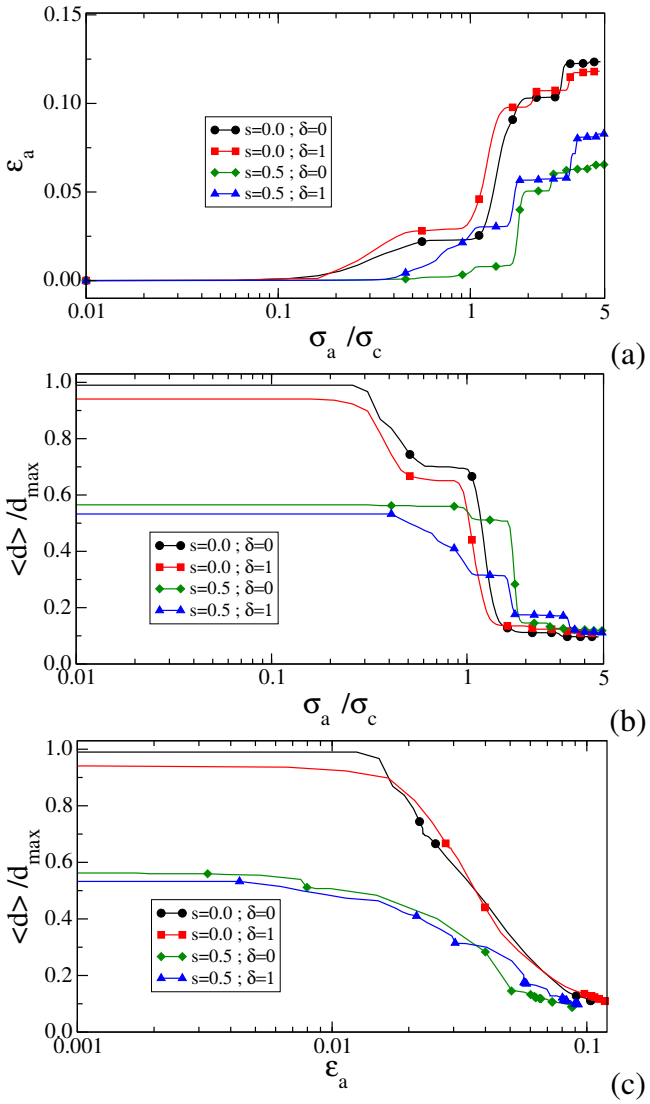

Figure 7: Evolution of axial deformation (a) and mean particle diameter (b) as a function of normalized axial stress, and evolution of mean particle diameter as a function of axial strain (c), for four different combinations of size polydispersity s and shape irregularity δ. The diameters are normalized by the largest particle diameter d_{max} before the beginning of fragmentation.

Figure 6 displays three snapshots of a packing composed of irregular pentagons at three stages of evolution of the particles and cracks between adjacent irreducible fragments, as well as the fragments generated. We see that the cracks are initiated in different parts of the packing and most of time they do not propagate to neighbouring particles. Instead, due to local load transfer, they lead to the shattering of a few particles whereas a number of particles are at the same time only superficially damaged.

Figure 7(a) shows the axial deformation ε_a as a function of the normalised axial stress σ_a/σ_c for four different combinations of size polydispersity s and shape irregularity δ. Since the particles are perfectly rigid, the axial deformation reflects the breakup of particles and partial filling of the pore space by small fragments. This process begins for a stress well below the cohesive strength σ_c of the particles as a result of broad force distribution in granular materials and concentration of forces in strong force chains. The deformation then proceeds by periods of fast fragmenta-

tion due to shattering instability and sudden increase of ε_a followed by periods of loading without fragmentation and deformation. Up to $\sigma_a = 5\sigma_c$, the total deformation is larger for monodisperse ($s = 0$) packings than for polydisperse packings ($s = 0.5$). Figure 7(b) shows the evolution of the mean particle diameter $\langle d \rangle$ normalized by d_{max} as a function of axial stress. The evolution of $\langle d \rangle$ clearly underlies the "staircase" aspect of the evolution of deformation with a series of equilibrium configurations separated by rearrangements allowed by particle breakage. This correlation is observed for all values of s and δ. As a result, when $\langle d \rangle$ is plotted vs. ε_a, we observe an almost smooth dependence as shown in Fig. 7(c). In the monodisperse case, the mean particle size declines logarithmically with axial deformation during fragmentation. In the polydisperse case, we observe a similar trend but over a narrower range. Note that for all values of s and δ, the mean particle diameter is two times the diameter of a irreducible fragment at $\sigma_a = 5\sigma_c$.

Figure 8 shows the cumulative volume fraction (CVF) $h(d)$ of fragmented particles at different levels of compression for packings of regular monodisperse (($s = 0.0$) and polydisperse ($s = 0.5$) particles. By definition, we have $h(d) = \pi \sum_{d_i<d} d_i^2 n(d_i)\, \delta d$, where $n(d_i)\delta d$ is the proportion of particles of diameter d_i. In the monodisperse case, the fragmentation generates quite rapidly all size classes down to the size of irreducible fragments. The CVF tends to a well-defined shape with three distinct size ranges: 1) small-size range $d < 0.1 d_{max}$, 2) intermediate range $0.1 d_{max} < d < 0.8 d_{max}$ and 3) large-size $d > 0.8 d_{max}$. The small-size range reflects the cutoff imposed by the size of irreducible fragments. The large-size range, with its relatively higher number of particles, represents a signature of the initial size distribution. It indicates that large particles break to a lesser extent due to the effect of smaller fragmented particles that tend to reduce the concentration of shear stresses.

The CVF in the intermediate range is nearly linear, implying thus a power-law distribution $n(d) \propto d^{\alpha}$ with $\alpha \simeq -2$. Note that this distribution corresponds to a uniform distribution by volume fractions and it was found to be the distribution best filling the pore space in two dimensions (Voivret, Radjaï, Delenne, & Youssoufi 2007). This distribution is also very close to the fractal distribution of Apollonian packings with exponent $\alpha \simeq -2.3$ (Astrom & Herrmann 1998). The emergence of a pore-filling power-law size distribution by fragmentation is remarkable as it suggests that the particle breakup down to small sizes is affected by the sizes of unfilled pores. As far as this is the case, the size distribution is stable and only the low-limit particle size evolves. The case of polydisperse packings, shown in Fig. 8(b), is interesting in this respect. Here, the initial size distribution is uniform by volume fractions from the very beginning. We see that the linear CVF is conserved by fragmentation in the range $d > 0.3 d_{max}$.

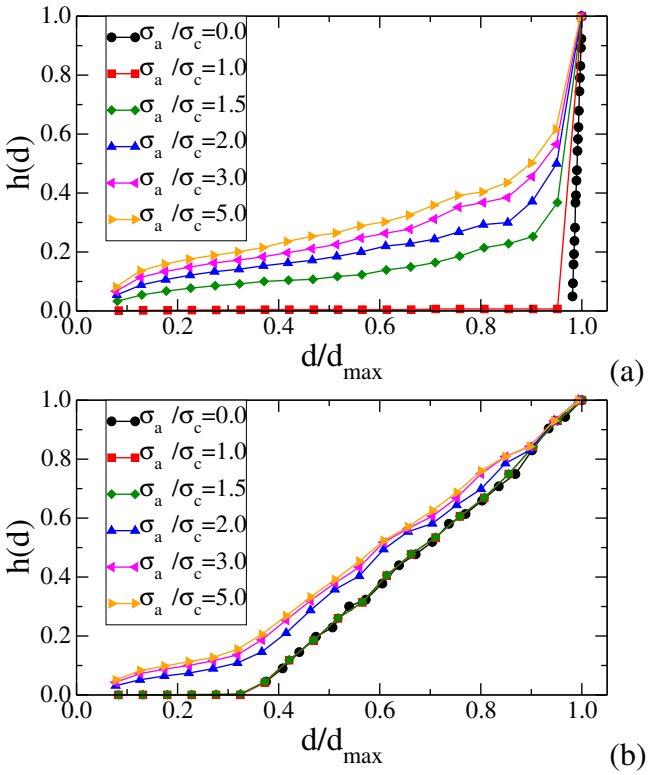

Figure 8: Cumulative volume fraction of particles during compression for packings of regular ($\delta = 0$) pentagons both monodisperse ($s = 0.0$) (a) and polydisperse with ($s = 0.5$)(b). The diameters are normalized by the diameter d_{max} of the largest particle before the beginning of particle breakage.

4 CONCLUSION

In this work, we introduced a numerical approach based on the contact dynamics method and meshing of the particles by irreducible fragments of polygonal shape for the simulation of granular materials with potential particle breakup. This approach conserves particle shapes (polygonal) and total volume of the particles during the fragmentation process. The fracture threshold of a single particle scales with its cohesive strength and is not affected by the number of meshes if the latter is sufficiently high. It was shown that stress-controlled oedometric compaction of crushable particles occurs in consecutive periods of intense particle breakup leading to rearrangements and fast increase of packing fraction, and periods of loading with nearly no particle breakup. The fragmentation process is initiated by cracks inside the particles. The cracks do not propagate from particle to particle. Instead, local shattering of a number of particles occurs as a result of the effect of persistent strong force chains. We showed that the cumulative volume fractions are linear in the intermediate size range, corresponding to a power-law size distribution of exponent -2. More work is under way to characterize in more detail the fragmentation process, the evolution of local stresses and contact force distributions, the shapes of fragments, and the effect of external parameters such as gravity. In the same way, an interesting topic that may be investigated within the present approach is the effect of particle breakup on the quasi-static and inertial granular flows.

REFERENCES

Abe, S. & K. Mair (2009). Effects of gouge fragment shape on fault friction: New 3d modelling results. *Geophysical Research Letters 36*(23), n/a–n/a.

Agnolin, I. & J.-N. Roux (2007, Dec). Internal states of model isotropic granular packings. i. assembling process, geometry, and contact networks. *Phys. Rev. E 76*, 061302.

Astrom, J. & H. Herrmann (1998). Fragmentation of grains in a two-dimensional packing. *The European Physical Journal B - Condensed Matter and Complex Systems 5*(3), 551–554.

Azéma, E. & F. Radjaï (2010). Stress-strain behavior and geometrical properties of packings of elongated particles. *Phys. Rev. E 81*, 051304.

Azéma, E. & F. Radjaï(2012). Force chains and contact network topology in sheared packings of elongated particles. *Phys. Rev. E 85*, 031303.

Azéma, E., F. Radjaï, & F. Dubois (2013). Packings of irregular polyhedral particles: strength, structure and effects of angularity. *Phys. Rev. E 87*, 062203.

Azéma, E., F. Radjaï, R. Peyroux, & G. Saussine (2007). Force transmission in a packing of pentagonal particles. *Phys. Rev. E 76*(1), 011301.

Azéma, E., F. Radjaï, & G. Saussine (2009). Quasistatic rheology, force transmission and fabric properties of a packing of irregular polyhedral particles. *Mechanics of Materials 41*, 721–741.

Ben-Nun, O., I. Einav, & A. Tordesillas (2010, Mar). Force attractor in confined comminution of granular materials. *Phys. Rev. Lett. 104*, 108001.

Bird, N., C. Watts, A. Tarquis, & A. Whitmore (2009). Modeling dynamic fragmentation of soil. *Vadose Zone Journal 8*(1), 197–201.

Bolton, M. D., . Y. N. 2, & Y. P. Cheng (2008). Micro- and macro-mechanical behaviour of dem crushable materials. *Géotechnique 58*, 471–480.

Cheng, Y. P., M. D. Bolton, & Y. Nakata (2004). Crushing and plastic deformation of soils simulated using dem. *Géotechnique 54*, 131–141(10).

Cleary, P. (2001). Recent advances in dem modelling of tumbling mills. *Minerals Engineering 14*(10), 1295 – 1319.

Couroyer, C., Z. Ning, & M. Ghadiri (2000). Distinct element analysis of bulk crushing: effect of particle properties and loading rate. *Powder Technology 109*, 241 – 254.

D'Addetta, G., F. Kun, & E. Ramm (2002). On the application of a discrete model to the fracture process of cohesive granular materials. *Granular Matter 4*(2), 77–90.

Das, A., G. D. Nguyen, & I. Einav (2011). Compaction bands due to grain crushing in porous rocks: a theoretical approach based on breakage mechanics. *Journal of Geophysical Research: Solid Earth (1978–2012) 116*(B8).

Elek, P. & S. Jaramaz (2009). Fragment mass distribution of naturally fragmenting warheads. *FME Transactions 37*(3), 129–135.

Esnault, V. & J.-N. Roux (2013). 3d numerical simulation study of quasistatic grinding process on a model granular material. *Mechanics of Materials 66*(0), 88 – 109.

Fuerstenau, D., O. Gutsche, & P. Kapur (1996). Confined particle bed comminution under compressive loads. In K. Forssberg and K. Schnert (Eds.), *Comminution 1994*, pp. 521 – 537. Amsterdam: Elsevier.

Galindo-Torres, S., D. Pedroso, D. Williams, & L. Li (2012). Breaking processes in three-dimensional bonded granular materials with general shapes. *Computer Physics Communications 183*(2), 266 – 277.

Gorokhovski, M. (2003). Fragmentation under the scaling symmetry and turbulent cascade with intermittency. Technical report, DTIC Document.

Hosten, C. & H. Cimilli (2009). The effects of feed size distribution on confined-bed comminution of quartz and calcite in piston-die press. *International Journal of Mineral Processing 91*, 81 – 87.

Khanal, M., W. Schubert, & J. Tomas (2007). Discrete element method simulation of bed comminution. *Minerals Engineering 20*(2), 179 – 187.

Liu, L., K. Kafui, & C. Thornton (2010). Impact breakage of spherical, cuboidal and cylindrical agglomerates. *Powder Technology 199*(2), 189 – 196.

Metzger, M. J. & B. J. Glasser (2012). Numerical investigation of the breakage of bonded agglomerates during impact. *Powder Technology 217*(0), 304 – 314.

Moreau, J. (1994). Some numerical methods in multibody dynamics : application to granular. *European J. Mech. A Solids 13*, 93–114.

Moreno, R., M. Ghadiri, & S. Antony (2003). Effect of the impact angle on the breakage of agglomerates: a numerical study using dem. *Powder Technology 130*(1-3), 132 – 137.

Nakata, Y., M. Hyodo, A. F. Hyde, Y. Kato, & H. Murata (2001). Microscopic particle crushing of sand subjected to high pressure one-dimensional compression. *Soils and foundations 41*(1), 69–82.

Potapov, A. V. & C. S. Campbell (2001). Parametric dependence of particle breakage mechanisms. *Powder Technology 120*(3), 164 – 174.

Radjaï, F. (1998). Multicontact dynamics. In H. J. H. et al. (Ed.), *Physics of Dry Granular Media*, Netherlands, pp. 305–312. Kluwer Academic Publishers.

Radjaï, F. & F. Dubois (March 2011). *Discrete Numerical Modeling of Granular Materials*. New-York: Wiley-ISTE. ISBN: 978-1-84821-260-2.

Radjaï, F. & V. Richefeu (2009). Contact dynamics as a nonsmooth discrete element method. *Mechanics of Materials 41*(6), 715 – 728. ¡ce:title¿Advances in the Dynamics of Granular Materials¡/ce:title¿.

Redner, S. (1990). Statistical theory of fragmentation. In *Disorder and Fracture*, pp. 31–48. Springer.

Thornton, C., M. T. Ciomocos, & M. J. Adams (2004). Numerical simulations of diametrical compression tests on agglomerates. *Powder Technology 140*, 258–267.

Thornton, C., K. K. Yin, & M. J. Adams (1996). Numerical simulation of the impact fracture and fragmentation of agglomerates. *J. Phys. D: Appl. Phys. 29*, 424–435.

Timár, G., F. Kun, H. A. Carmona, & H. J. Herrmann (2012, Jul). Scaling laws for impact fragmentation of spherical solids. *Phys. Rev. E 86*, 016113.

Tsoungui, O., D. Vallet, & J. Charmet (1999). Numerical model of crushing of grains inside two-dimensional granular materials. *Powder Technology 105*, 190 – 198.

Tsoungui, O., D. Vallet, J.-C. Charmet, & S. Roux (1997). Pression partielle par classe granulomtrique dans un empilement polydisperse. *Comptes Rendus de l'Acadmie des Sciences - Series IIB - Mechanics-Physics-Chemistry-Astronomy 325*(8), 457 – 464.

Voivret, C., F. Radjaï, J.-Y. Delenne, & M. E. Youssoufi (2007, Aug). Space-filling properties of polydisperse granular media. *Phys. Rev. E 76*, 021301.

Wang, J. & H. Yan (2012). Dem analysis of energy dissipation in crushable soils. *Soils and Foundations 52*(4), 644 – 657.

Wohletz, K., M. Sheridan, & W. Brown (1989). Particle size distributions and the sequential fragmentation/transport theory applied to volcanic ash. *Journal of Geophysical Research: Solid Earth (1978–2012) 94*(B11), 15703–15721.